



Novel antiinflammatory biologics shaped by parasite–host coevolution

Stephanie M. Ryan^{a,1}, Roland Ruscher^{a,1,2} , Wayne A. Johnston^b, Darren A. Pickering^a , Malcolm W. Kennedy^c , Brian O. Smith^d , Linda Jones^a, Geraldine Buitrago^a, Matt A. Field^a , Adrian J. Esterman^{a,e}, Connor P. McHugh^a, Daniel J. Browne^a, Martha M. Cooper^a , Rachael Y. M. Ryan^a, Denise L. Doolan^a , Christian R. Engwerda^f, Kim Miles^a, Makedonka Mitreva^g , John Croese^{a,h} , Tony Rahman^h, Kirill Alexandrov^b, Paul R. Giacomin^{a,2,3}, and Alex Loukas^{a,2,3}

Edited by Patricia Johnson, David Geffen School of Medicine at UCLA, Los Angeles, CA; received February 15, 2022; accepted August 4, 2022

Parasitic helminth infections, while a major cause of neglected tropical disease burden, negatively correlate with the incidence of immune-mediated inflammatory diseases such as inflammatory bowel diseases (IBD). To evade expulsion, helminths have developed sophisticated mechanisms to regulate their host's immune responses. Controlled experimental human helminth infections have been assessed clinically for treating inflammatory conditions; however, such a radical therapeutic modality has challenges. An alternative approach is to harness the immunomodulatory properties within the worm's excretory–secretory (ES) complement, its secretome. Here, we report a biologics discovery and validation pipeline to generate and screen *in vivo* a recombinant cell-free secretome library of helminth-derived immunomodulatory proteins. We successfully expressed 78 recombinant ES proteins from gastrointestinal hookworms and screened the crude *in vitro* translation reactions for anti-IBD properties in a mouse model of acute colitis. After statistical filtering and ranking, 20 proteins conferred significant protection against various parameters of colitis. Lead candidates from distinct protein families, including annexins, transthyretins, nematode-specific retinol-binding proteins, and SCP/TAPS were identified. Representative proteins were produced in mammalian cells and further validated, including *ex vivo* suppression of inflammatory cytokine secretion by T cells from IBD patient colon biopsies. Proteins identified herein offer promise as novel, safe, and mechanistically differentiated biologics for treating the globally increasing burden of inflammatory diseases.

hookworm | IBD | protein | therapeutic | helminth

Inflammatory bowel disease (IBD) includes debilitating conditions such as ulcerative colitis (UC) and Crohn's disease. IBD affects over 6 million people worldwide, with a higher incidence in industrialized compared to developing countries, although incidence is also rising in the latter due to increasing urbanization (1, 2). Currently used therapeutics to treat IBD include antibiotics, steroids, and antibodies against inflammatory cytokines such as tumor necrosis factor (TNF) or mucosal homing molecules such as integrin $\alpha_4\beta_7$ (3, 4). However, current treatment strategies can have serious off-target effects and often become ineffective over time, and there is currently no cure for IBD (5, 6). New and safer induction and maintenance therapies are desperately needed.

Intestinal parasitic helminths secrete a suite of bioactive molecules to avert and subvert host inflammatory responses directed at worm expulsion (7, 8). Such anti-inflammatory capacities shaped by evolutionary selection pressure have received growing attention due to their potential to treat inflammatory diseases. Controlled experimental helminth infections have been trialed in inflammatory intestinal conditions including IBD and celiac disease (9–12). Complimentary studies have shown that factors excreted or secreted (ES) by worms can have therapeutic effects similar to live worms. This has been demonstrated using either complex mixtures of naturally derived helminth ES (containing hundreds of potential immunomodulatory factors) or individual recombinant proteins (8, 13). However, these approaches are hindered by difficulties in scaling up and standardizing quantity, purity, and homogeneity of natural ES products. Similarly, efforts required to express individual proteins within a helminth's secretome (hundreds of proteins) and characterize their biological activities are prohibitive.

To tackle these challenges, we set out to design a high-throughput screening system to identify anti-inflammatory proteins and potential IBD drug leads within the secretome of a gut-dwelling hookworm.

Significance

Inflammatory bowel diseases (IBD) are on the rise. Many studies have highlighted an inverse correlation between infection with parasitic helminths and the incidence of immune-mediated inflammatory diseases, such as IBD. The mechanisms by which parasitic helminths suppress inflammation and prevent the onset of inflammatory diseases is not well understood. This study describes a discovery and validation pipeline of antiinflammatory biologics from the recombinant secretome of gut-dwelling hookworms as novel and safe drug leads. Numerous proteins from distinct families protected mice against inducible colitis, and lead proteins suppressed production of inflammatory cytokines from IBD patient gut biopsy T cells *ex vivo*, highlighting a gold mine of new biologics inspired by coevolution of humans and their macrobiome.

This article is a PNAS Direct Submission.

Copyright © 2022 the Author(s). Published by PNAS. This article is distributed under [Creative Commons Attribution-NonCommercial-NoDerivatives License 4.0 \(CC BY-NC-ND\)](https://creativecommons.org/licenses/by-nc-nd/4.0/).

¹S.M.R. and R.R. contributed equally to this work.

²To whom correspondence may be addressed. Email: roland.ruscher@jcu.edu.au, paul.giacomin@jcu.edu.au, or alex.loukas@jcu.edu.au.

³P.R.G. and A.L. contributed equally to this work.

This article contains supporting information online at <http://www.pnas.org/lookup/suppl/doi:10.1073/pnas.2202795119/-/DCSupplemental>.

Published August 29, 2022.

Results

Cell-Free Expression of Recombinant Hookworm ES Proteome.

Based on the published ES proteome and transcriptome of *Ancylostoma caninum* (14, 15), we compiled a list of 91 full-length protein-coding genes (SI Appendix, Table S1) from different protein families (Fig. 1A), focusing on molecules with a predicted signal peptide, and/or members of a protein family with previously reported interactions with mammalian tissues or inflammatory responses (Fig. 1A). The corresponding complementary DNAs (cDNAs) fused to an N-terminal enhanced green fluorescent protein (eGFP) tag were expressed in a *Leishmania tarentolae* in vitro translation system (LTE) (Fig. 1B–E). Of the

91 cDNA sequences, 78 proteins were successfully expressed as in vitro translation reactions (IVTRs) in this system.

Over 25% of the IVTRs Alleviate Defined Experimental Colitis Parameters. We next tested whether a single administration of the crude recombinant protein-containing IVTRs displayed efficacy in the 2,4,6-trinitrobenzene sulfonic acid (TNBS) model of acute colitis, which enabled high-throughput in vivo screening of our recombinant secretome (Fig. 2A–D). Mice were treated with IVTRs containing the hookworm protein of interest, or eGFP alone as a control, via intraperitoneal injection 1 d before TNBS administration or were left untreated (naïve). As expected, mice treated with IVTR containing eGFP

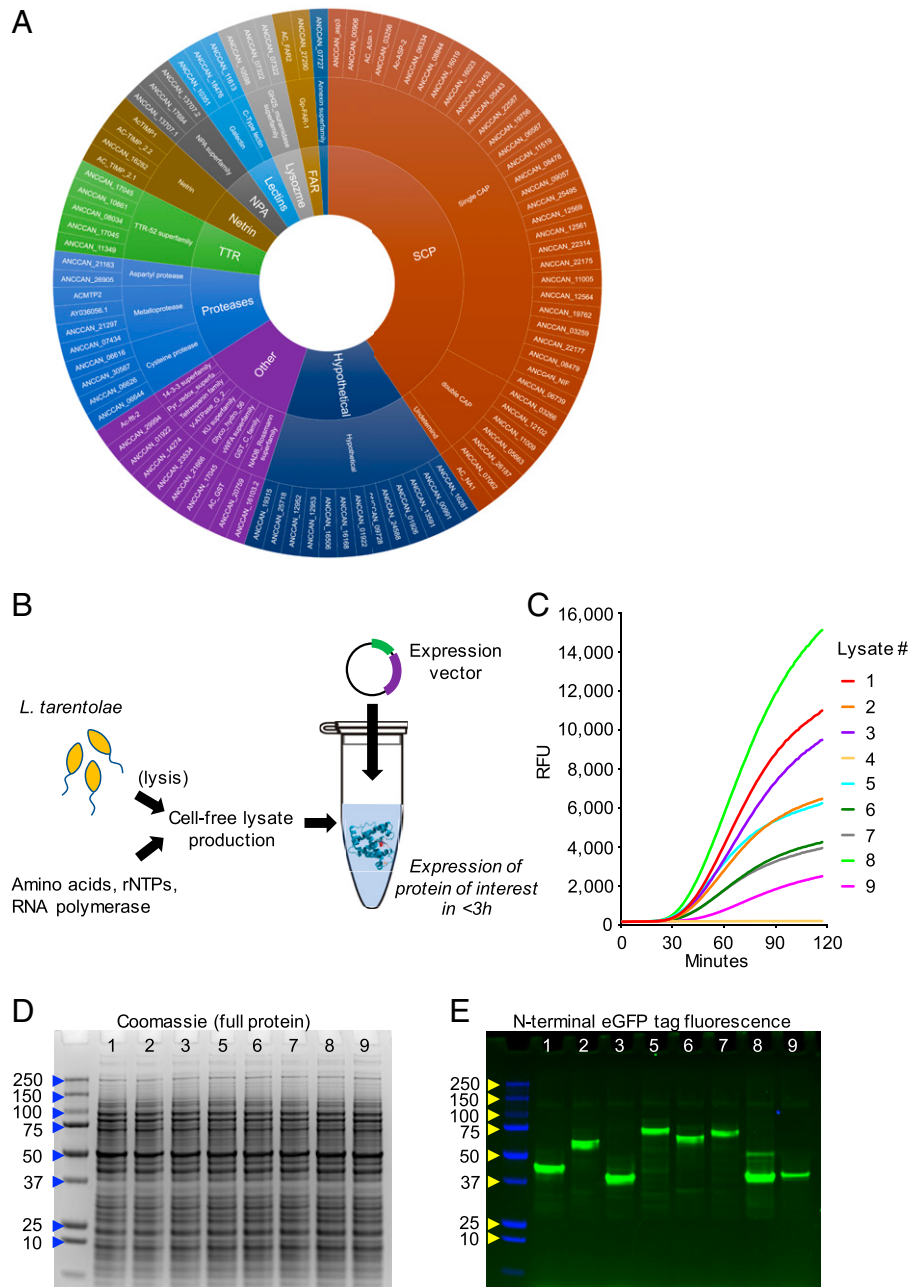


Fig. 1. Cell-free expression of recombinant hookworm ES proteome. (A) Predicted ES protein sequences were assembled into protein families (Pfam) using Blast2Go. Where Blast2Go did not assign a Pfam status, a manual BlastP search was performed. If manual searches did not assign a Pfam, the protein was deemed to be “hypothetical.” (B) Schematic depiction of the production of the hookworm cell-free secretome library using a *L. tarentolae* in vitro translation system. (C) Representative IVTRs of nine hookworm recombinant proteins fused to eGFP that were monitored over time by measuring the RFU. (D) Protein expression in IVTRs was visualized by Coomassie-stained SDS-PAGE gel loaded with IVTRs shown in B. (E) The same gel as shown in D but scanned for eGFP fluorescence. The fluorescent bands represent eGFP fluorescence of hookworm recombinant proteins.

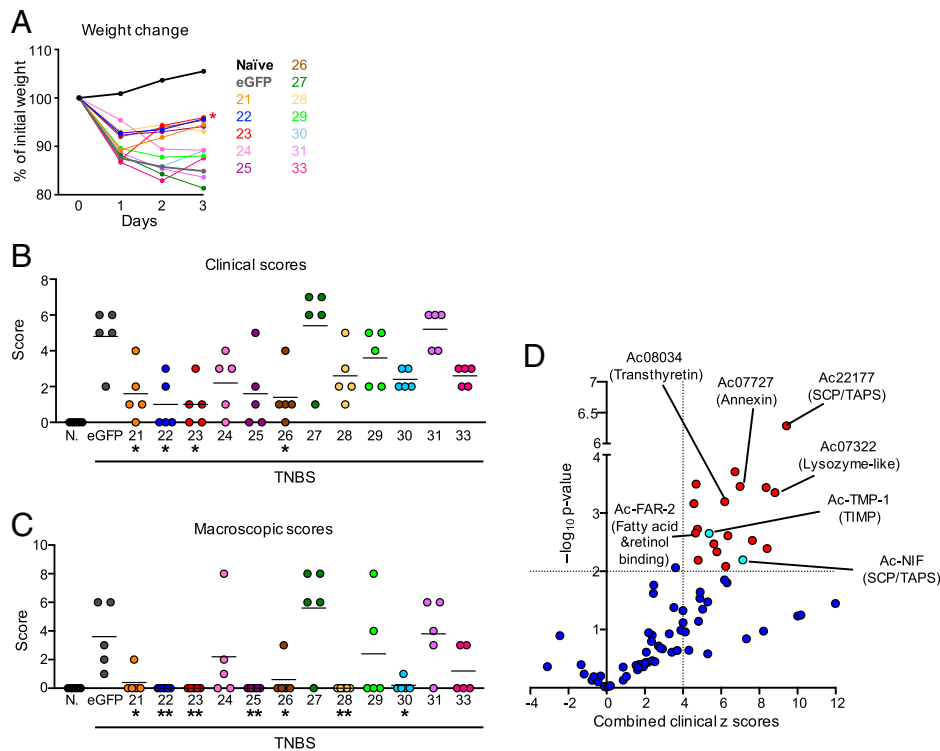


Fig. 2. Twenty of the tested IVTRs alleviated experimental colitis. BALB/c mice were injected intraperitoneally with 200 μ L of IVTRs (protein concentration: 100 μ g/mL) 1 d prior to intrarectal administration of TNBS and were monitored daily for 3 d before mice were killed. $n =$ naïve. (A) Mean percent change of initial weight from a representative experiment where 12 IVTRs containing different hookworm proteins fused to eGFP were screened for activity compared to eGFP-only IVTR control and naïve mice ($n = 5$ per group). (B) Clinical scores (mean and individual data points) combining fecal consistency, motility, piloerection and weight change at day 3. (C) Macroscopic colon pathology scores (mean and individual data points) at day-3 necropsy. * $P \leq 0.05$, ** $P \leq 0.01$, Mann-Whitney U test compared to eGFP control. (D) Combined statistical analyses of the efficacy of all 78 expressed hookworm protein-containing IVTRs compared to respective eGFP-IVTR control. The x axis depicts the difference in mean of the combined z-scores of clinical outcomes (weight loss, colon length, clinical scores, and macroscopic scores) between treatment and control (eGFP IVTR), and the y axis shows the P value where $P < 0.01$ or $-\log_{10} > 2$ were regarded as significant. Proteins that achieved significant protection in both categories are highlighted in red (or turquoise) and were selected for further validation, whereas proteins that failed to achieve significant protection in both categories are shown in dark blue. Proteins shown in turquoise have previously been reported (in purified recombinant form) to alleviate experimental colitis. The proteins that were subsequently expressed in mammalian cells are annotated with their protein name and Pfam status.

alone prior to TNBS administration exhibited rapid weight loss (Fig. 2A), elevated clinical scores (Fig. 2B), and macroscopic pathology scores (Fig. 2C) compared to naïve mice. In a representative experiment where 12 randomly selected hookworm protein-containing IVTRs were screened, we observed that one IVTR (#23) was able to reduce all three disease parameters (Fig. 2A–C), while six other IVTRs reduced either clinical score or macroscopic colon pathology (Fig. 2B and C). We then generated combined clinical Z-scores to rank and compare the effects of each of the 78 hookworm protein-containing IVTRs across all screening experiments, based on the four disease outcomes (weight change, clinical score, macroscopic pathology, and colon length). This resulted in an overall difference of means score and a P value for each protein compared to eGFP control, which we used to rank the proteins and identify 20 proteins that displayed significant protection in the TNBS colitis model. These 20 proteins became our lead therapeutic candidates for further testing and validation and included 12 members of the Sperm-Coating Protein/Tpx-1/Ag5/PR-1/Sc7 (SCP-TAPS) superfamily, two transthyretins (TTR), a nematode-specific fatty acid and retinol-binding protein (FAR), two homologs of tissue inhibitor of metalloproteinase (TIMP), a lysozyme, an annexin, and a hypothetical protein (Fig. 2D and Table 1). Of note, two of the identified candidates—the TIMP-like netrin domain-containing protein Ac-TMP-1 (Ac-AIP-1) and Ac-NIF (a SCP protein)—had been previously reported to display efficacy in mouse models of colitis, thereby independently validating our approach (16, 17).

Expression of Efficacious IVTR Proteins in Mammalian Cells and Validation. In vitro translation products are not readily scalable for preclinical and clinical studies, so we took 8 of the top 10 most efficacious IVTR candidates—ensuring that all protein families were represented and avoiding redundancy in the heavily represented SCP/TAPS family—and expressed them in Expi293F human embryonic kidney cells and purified the recombinant proteins. Five of the proteins (Ac07322, Ac08034, Ac07727, Ac22177, and Ac-FAR-2) were successfully produced and purified in sufficient quantities to test in the TNBS colitis model and to explore the impact of coculturing the purified proteins ex vivo with colon biopsies from UC patients.

We assessed the efficacy of the five mammalian-cell-produced recombinant proteins in the TNBS colitis model, compared to phosphate-buffered saline (PBS) vehicle control and an irrelevant control protein (bovine serum albumin, BSA) that was expressed and purified in identical fashion. As expected, PBS vehicle-treated mice displayed weight loss, elevated clinical scores, and macroscopic pathology scores after TNBS administration, and this was not affected by cotreatment with the negative control recombinant BSA (Fig. 3A–C). Critically, of the five tested hookworm proteins, the transthyretin Ac08034 and the annexin Ac07727 were able to significantly limit weight loss, clinical scores, and macroscopic scores, while Ac-FAR-2 and Ac22177 significantly suppressed at least one disease parameter compared to control mice (Fig. 3A–C).

Table 1. Top-ranked proteins from TNBS colitis screen of hookworm IVTRs

Rank	IVTR ID	Gene name	Protein family
1	13	ANCCAN_22177	Sperm Coating Protein/Tpx-1/Ag5/PR-1/Sc7 (SCP/TAPS)
2	85	ANCCAN_00478 (Ac-ASP-2)	SCP/TAPS
3	23	ANCCAN_12569	SCP/TAPS
4	80	ANCCAN_07727	Annexin
5	16	ANCCAN_12564	SCP/TAPS
6	2	ANCCAN_07322	Lysozyme
7	70	ANCCAN_08034	Transthyretin (TTR)-52
8	22	ANCCAN_26187	SCP/TAPS
9	19	ANCCAN_07062	SCP/TAPS
10	79	ANCCAN_10127 (Ac-FAR-2)	Fatty acid and retinol-binding (FAR)
11	73	ANCCAN_13497 (Ac-TMP-1/Ac-AIP-1)	Tissue Inhibitor of Metalloprotease (TIMP)
12	83	ANCCAN_01926	No putative conserved domains
13	15	ANCCAN_19762	SCP/TAPS
14	72	ANCCAN_17044	TTR-52
15	9	ANCCAN_06741	SCP/TAPS
16	74	ANCCAN_16282	TIMP
17	11	ANCCAN_04194 (Ac-NIF)	SCP/TAPS
18	21	ANCCAN_12561	SCP/TAPS
19	17	ANCCAN_11005	SCP/TAPS
20	28	ANCCAN_11519	SCP/TAPS

The list includes the 20 top-ranked proteins in order of performance in the TNBS colitis screen and includes the rank (left column), IVTR ID (middle left column), gene name and protein name if known (middle right column), and protein family (right column). Gene accession codes (ANCCAN number) correspond to entries in Nematode.net (www.nematode.net/NN3_frontpage.cgi); where a gene has been previously reported in a publication, its gene name is also provided in parentheses.

Bioactivity of Five Proteins in Intestinal T Cells from Colitis Patients.

To assess potential translational value, we tested whether the five lead recombinant proteins produced in Expi293F cells displayed bioactivity against gut immune cells from UC patients. Twelve clinically diagnosed patients with UC, who were not currently taking other biologic therapies, were recruited to the study. Details of the participants are included in *SI Appendix, Table S2*. Fresh colon biopsies taken from noninflamed regions of gut tissue were collected, and single-cell suspensions of intraepithelial and lamina propria lymphocytes were isolated. Since T cells are one of the major immune cell subsets involved in IBD progression (18, 19),

we examined whether the hookworm proteins could suppress cytokine responses from T cells stimulated *ex vivo* with T cell receptor (TCR) engaging anti-CD3 and anti-CD28 coated beads (Fig. 4 A–D). Responses were compared to unstimulated cells cultured with PBS alone, or cells cultured with TCR stimulation and either PBS vehicle only, the negative control protein BSA, or the positive control cyclosporine A (CSA). To account for patient-to-patient variability, each dataset (per patient) was normalized to the PBS + anti-CD3/CD28 bead stimulated condition, as indicated by the dotted lines (100%) in the graphs. Analysis of culture supernatants using a bead-based multiplex assay to detect human inflammatory cytokines

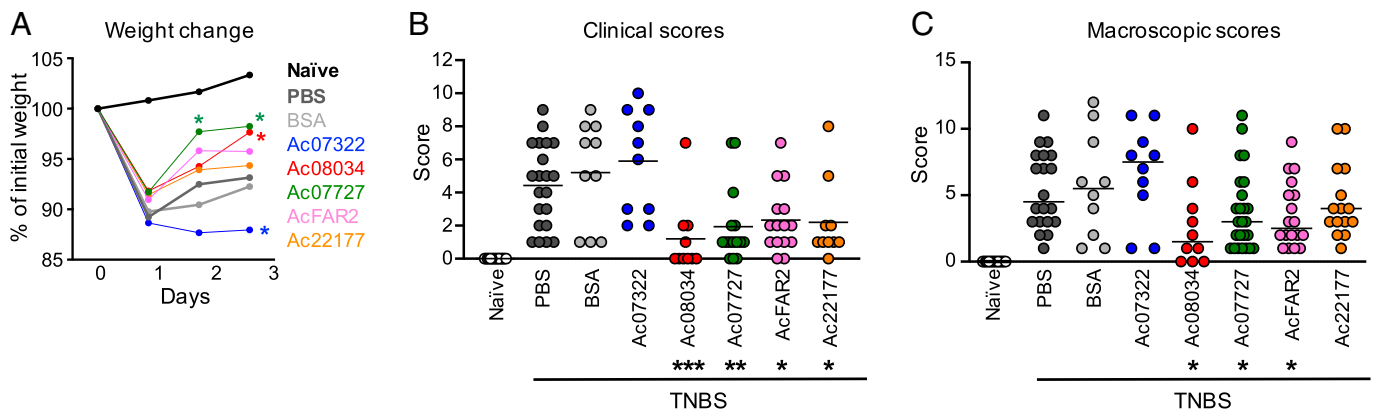


Fig. 3. Validation of efficacious proteins in TNBS colitis after expression in mammalian cells. BALB/c mice were injected intraperitoneally with 20 μ g of recombinant hookworm proteins generated in Expi293F human embryonic kidney cells 1 d prior to intrarectal administration of TNBS and daily thereafter until termination. Control mice received either recombinant BSA expressed using the same production methods or PBS vehicle. (A) Mean percent change of initial weight. (B) Clinical scores (mean and individual data points). (C) Macroscopic scores of colon pathology (mean and individual data points). Data are combined from three individual experiments, where $n = 10$ to 20 for each treatment group. $*P \leq 0.05$, $**P \leq 0.01$, $***P \leq 0.001$, Mann-Whitney U test compared to PBS control.

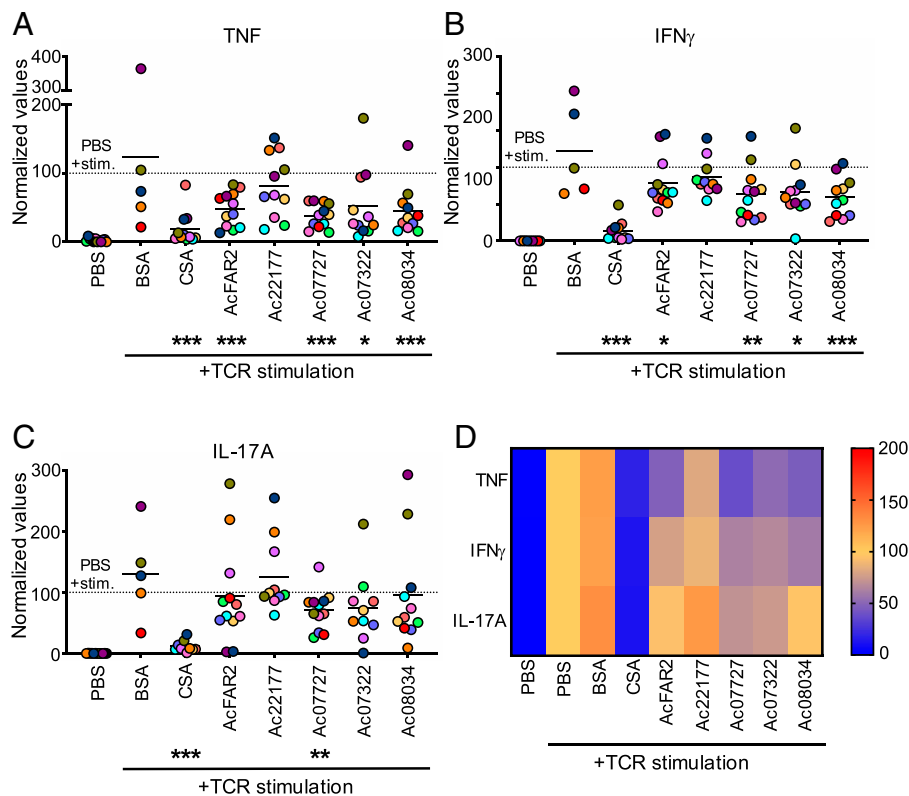


Fig. 4. Lead proteins reduce inflammatory cytokine release by intestinal T cells from human colitis patients. Intraepithelial lymphocytes and lamina propria cells were isolated and combined from fresh colon biopsies collected from UC patients. Cells were treated with either PBS control, purified recombinant hookworm proteins, or bovine serum albumin, generated in Expi293F cells, and then stimulated with α CD3/CD28 Dynabeads (TCR stimulation). Patient-to-patient variability was accounted for by normalizing all data to the PBS (vehicle)-treated samples (100%, indicated by a dotted line in Fig. 4 A–C). Ac-FAR-2 was used at 10 μ g/mL based on earlier studies in our laboratory, and all other proteins at 50 μ g/mL. Positive control cells were treated with CSA or were left unstimulated (PBS). (A–C) Cell-free supernatants were collected and analyzed after 3 d of culture for TNF, IFN γ , and IL-17A secretion. Values were normalized to PBS-treated and stimulated conditions for each respective patient (dotted line). Data are combined from two independent sample collection days, with each colored symbol representing an individual patient sample ($n = 5$ to 12 per treatment group) and the mean value for each treatment shown as a horizontal line. (D) Heat map depicting the combined mean cytokine values from A–C. * $P \leq 0.05$, ** $P \leq 0.01$, *** $P \leq 0.001$, one-sample t test.

revealed that TCR stimulation in the presence of PBS alone led to secretion of the IBD-relevant cytokines TNF, interferon (IFN)- γ , and interleukin (IL)-17A, and this response was unaffected by cotreatment with BSA control and was significantly suppressed by CSA (Fig. 4 A–C). Interestingly, Ac07727 significantly reduced the secretion of all three of these cytokines, while Ac07322 (despite not protecting in TNBS colitis when expressed in Expi293F cells), Ac-FAR-2, and Ac08034 were able to suppress secretion of at least two of the inflammatory cytokines (Fig. 4 A–C). One of the proteins (Ac22177) did not significantly suppress secretion of any of the cytokines, in part because of the influence of “nonresponding” outlier patients (Fig. 4 A–C and *SI Appendix, Table S2*). A summary of the efficacy of the six hookworm proteins is presented in Fig. 4D, highlighting that similar to our animal studies (Fig. 3) the proteins Ac-FAR-2, Ac07727, and Ac08034 were the strongest performers when tested on human UC patient colon T cells (Fig. 4). None of the lead proteins tested for cytotoxicity with human peripheral blood mononuclear cells (PBMC) showed any signs of toxicity at a range of concentrations spanning those used for the colon biopsy study (*SI Appendix, Fig. S1*).

Ac-FAR-2 Binds Hydrophobic Ligands. Finally, we aimed to shed some light on possible mechanisms of action (MoA) of select lead proteins. Ac-FAR-2, Ac07727, Ac22177, and Ac08034 belong to structurally disparate protein families but share an association with lipid/retinol binding and/or signaling (20–22), highlighting one pathway by which gastrointestinal helminths

may confer substantial immunoregulatory activity (23, 24). To test this possibility in more depth, we performed a fluorescence-based ligand binding analysis using *all-trans* retinol and fatty acid probes. Ac-FAR-2 substantially increased retinol’s fluorescence emission (Fig. 5A), indicative of entry into a binding site in the protein that shields it from solvent water. Retinol was partially displaced competitively by oleic acid (Fig. 5A, indicated by reduced fluorescence intensity), suggesting that the retinol binding site is congruent or overlapping with a site for fatty acids. We explored this further using a saturated fatty acid tagged with an environment-sensitive fluorophore, 11-[5-(dimethylamino)-1-naphthalenesulfonylamino]undecanoic acid (DAUDA). Ac-FAR-2 not only produced a substantial increase in DAUDA’s fluorescence emission but also a blue shift in peak emission from 532 nm to 483 nm (Fig. 5B), a shift that indicates entry into a strongly apolar binding site environment. DAUDA was readily displaced from Ac-FAR-2’s binding site by arachidonic acid (Fig. 5B), a precursor of eicosanoids that are active in inflammation and immune responses (25). Binding of fatty acids was further confirmed using the intrinsically fluorescent natural, unmodified fatty acid, *cis*-parinaric acid (cPnA) (*SI Appendix, Fig. S2A*).

We next tested the binding of retinol or DAUDA for our three lead proteins side by side and found that Ac-FAR-2, but not Ac07727, Ac22177, or Ac08034, bound these lipids (Fig. 5 C and D), and this was also true for the binding of cPnA (*SI Appendix, Fig. S2B*). Finally, we tested whether these proteins may possess binding sites for different classes of hydrophobic molecule by using a fluorescent probe that binds nonspecifically

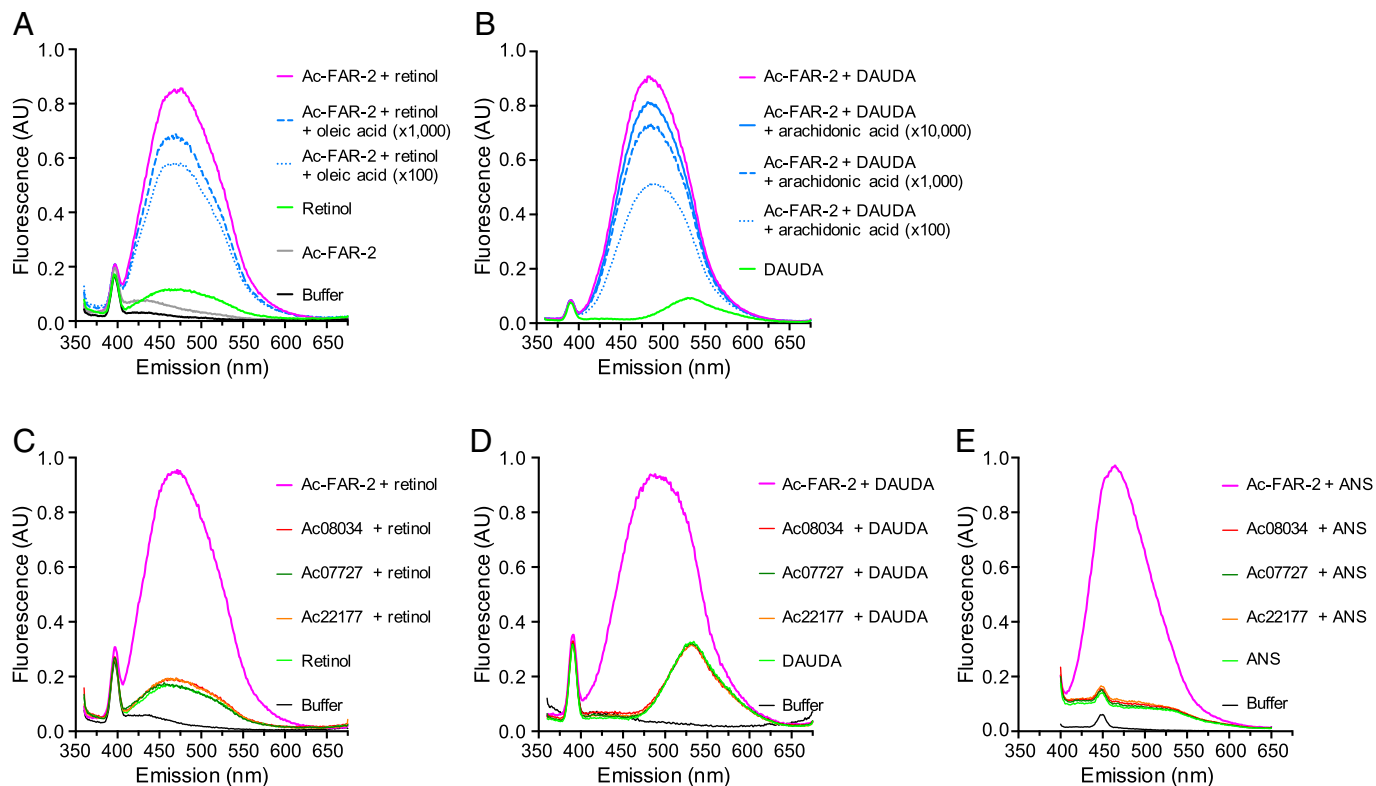


Fig. 5. Ac-FAR-2 binds hydrophobic ligands. Binding was assessed by spectrofluorometric analysis. (A) Binding of *all-trans* retinol to Ac-FAR-2, with no or competitive displacement with successive additions of 10-fold increasing concentrations of oleic acid. (B) Binding of DAUDA to Ac-FAR-2, with no or successive additions of 10-fold increasing concentrations of arachidonic acid. (C and D) Failure of individual lead proteins Ac08034, Ac22177, and Ac07727 to bind *all-trans* retinol (C), DAUDA (D), or ANS (E) compared with Ac-FAR-2. Fluorescence intensity was converted to relative arbitrary units (AU). The small sharp peaks at shorter wavelengths are from water Raman scatter.

to apolar surfaces or pockets in proteins, 8-anilino-1-naphthalenesulfonic acid (ANS). Importantly, while we did not observe binding of ANS to Ac07727, Ac22177, or Ac08034, Ac-FAR-2 demonstrated clear binding of this molecule (Fig. 5E). While ANS will likely enter a retinol or fatty acid-binding pocket, this could equally indicate that Ac-FAR-2 may bind a range of hydrophobic molecules beyond the suspected function of binding retinol and fatty acids.

Discussion

Overall, our *in vivo/ex vivo* screening platform enabled the identification of three distinct lead proteins (Ac-FAR-2, Ac07727, and Ac08034), from a starting pool of 78, that alleviated disease outcome in experimental colitis and, importantly, significantly reduced inflammatory cytokine release by intestinal T cells from UC patients. None of these protein families had previously been reported to have antiinflammatory properties when produced by helminths. It is noteworthy that members of some of these protein families have been implicated in antiinflammatory processes, but mostly through the overexpression (or absence) of endogenous protein in inflamed tissues. For example, annexin A1 (the family to which Ac07727 belongs) replicates many of the described antiinflammatory effects of glucocorticoids and is overexpressed in inflamed gut tissue, where it acts as a proresolving mediator of wound healing (26). Moreover, intestinal delivery of a nanoparticle-encapsulated annexin A1 peptide mimetic accelerated mucosal healing and accelerated recovery from inducible colitis in mice (27), and annexin A1-deficient mice are more resistant to anti-TNF treatment in dextran sulfate sodium-induced colitis than wild-type controls (28). Ac-FAR-2 belongs to a

nematode-specific family of fatty acid-binding proteins, and its homolog Ac-FAR-1 binds to retinol (29). An antiinflammatory role for this protein family has not been reported until now, and it might sequester extracellular retinol and prevent its binding to serum amyloid A and/or block its receptor-mediated uptake into myeloid cells, thereby interfering with gut trafficking of lymphocytes and adaptive immune processes that may contribute to inflammation (30, 31). Indeed, our study confirms the capacity of Ac-FAR-2 to bind not only retinol and fatty acids but also a nonspecific hydrophobic probe, indicative of a potential MoA through such activities. Further, according to our findings, Ac-FAR-2 binds at least two classes of lipids (retinol and arachidonic acid) that are precursors of biologically active lipids such as retinoids and eicosanoids, including leukotrienes and prostaglandins. Leukotrienes and prostaglandins are known to play a role in inflammatory processes, and indeed some antiinflammatory drugs act through blocking the synthesis or inhibiting receptor binding by these molecules (25). While we have shed light on the MoA of Ac-FAR-2, it is clearly important moving forward to prioritize mechanistic studies of the remaining lead proteins and understand how they exert their respective antiinflammatory functions.

Genes encoding SCP/TAPS proteins accounted for 12 of the 20 proteins identified in our initial *in vivo* colitis screen. SCP/TAPS proteins are massively expanded in the genomes of hookworms and other gastrointestinal helminths, but little is known about their functions (32). Two of these SCP/TAPS proteins were Neutrophil Inhibitory Factor (NIF) and ASP-2, and both of these proteins have been shown to bind to human cell-surface proteins involved in inflammatory pathways (33, 34). Intriguingly, a secreted SCP/TAPS protein from the gastrointestinal

nematode *Heligmosomoides polygyrus* binds to sterols, highlighting the diverse array of ligands (lipids in particular) and possible functions of this important family of proteins (35). It should be noted, however, that Ac22177, the best-performing SCP/TAPS family member in the mouse colitis study, did not bind retinol or the lipids tested herein.

A limitation of the current study is that we focused on colitis as a model of inflammatory disorder. The TNBS colitis model has been suggested to be a better model for Crohn's disease than UC. However, the rationale of our study was to rapidly screen *in vivo* a large number of molecules for their efficacy in gut inflammation, so the rapid onset of inflammation in the TNBS model was ideal in this scenario. In line with this, colon biopsies from UC patients were readily available. Future studies, however, should evaluate our lead proteins in additional models of gut inflammation as well as in small intestinal biopsies from Crohn's disease patients. Further, elucidation of the therapeutic and prophylactic efficacy of our lead proteins in other immune-mediated inflammatory diseases with shared common pathogenic cells and pathways and in clinical settings should be performed in the future (36). Their mechanisms of action, including putative receptors they engage and the molecular pathways affected, are likely to be differentiated from existing therapeutic strategies given the coevolutionary nature of the host–parasite relationship. Moreover, the relative safety and tolerability of experimental hookworm infection (7) suggests that therapies based on these secreted proteins are likely to be safe and well-tolerated.

Importantly, our approach employing *in vivo* administration of IVTRs to mice experiencing inducible colitis can be applied to drug discovery from the secretomes of other organisms, particularly where there are limited quantities of crude starting material. Hookworms secrete a broad arsenal of proteins into the gut, and our findings emphasize the diversity of structures that appear to converge upon a common theme of lipid and retinoid binding to suppress inflammation. This work highlights the value of parasitic helminths as both a source of next-generation biologics as well as a tool for druggable target/pathway discovery guided by millennia of host–parasite coevolution.

Materials and Methods

Study Design. The overarching goal of the study was to generate a bank of recombinant hookworm secreted proteins expressed as IVTRs for an initial *in vivo* screen in a mouse model of acute colitis. These crude IVTRs allowed us to rapidly generate small quantities of recombinant proteins fused to eGFP in a eukaryotic cell-free system. Importantly, we controlled each mouse colitis study with a group that received IVTR containing recombinant eGFP alone. Sample sizes for colitis studies were determined on the basis of previous experience and statistical analyses, with a view to this first experiment being a high-throughput initial screen. Standard measurements were used in the TNBS model of acute colitis to determine efficacy, including weight change, clinical score, and macroscopic pathology score in a manner that enabled us to screen many test proteins. Lead proteins identified from the *in vivo* colitis screen of IVTRs were then expressed in mammalian cell lines and purified to ensure that proteins were produced in a way that is amenable to preclinical and ultimately clinical development. For the human component of our study, 12 UC patients were recruited, including men and women. Gut biopsy tissue was cultured with purified lead proteins expressed in mammalian cells, and modulation of T cell cytokine production was assessed. Sample sizes, replicates, and statistical measurements are included in the figures and legends and in the text where appropriate.

Mouse. Male and female specific pathogen free (SPF) BALB/cArc mice were purchased from the Animal Resources Centre and used at 5 to 10 wk of age. The animals were maintained in SPF conditions and rested for minimum 7 d

between arrival at our facilities and experiments. All experiments were approved by the James Cook University Animal Ethics Committee, and in compliance with the National Health and Medical Research Council Australian Code for the Care of Animals for Scientific purposes and the Queensland Animal Care and Protection Act.

Protein Selection. A total of 78 *A. caninum* ES proteins for IVTR recombinant expression were selected from Mulvenna et al. (15) based on their detection in adult worm ES products using liquid chromatography tandem mass spectrometry. The remaining 13 proteins were selected from the most highly up-regulated messenger RNA sequences corresponding to secreted proteins from the transcriptome of serum-activated infective third-stage larvae (as opposed to nonactivated larvae) as described by Datu et al. (14). Where PacBio cDNA sequences were partial and did not contain the full open reading frame (ORF), cDNAs were aligned to the reference genome in WormBase ParaSite (<https://parasite.wormbase.org/index.html>) to obtain complete ORFs.

Cell-Free Recombinant Protein Expression. ORFs with signal peptide-encoding regions removed were synthesized by Protein CT Biotechnologies with incorporation of KpnI and HindIII 5' and 3' restriction sites, respectively, to facilitate cloning into pLTE-GFP-3C and cell-free expression in *L. tarentolae* lysates as described (37). The cloning strategy ensured that recombinant proteins contained an N-terminal eGFP tag fused to the C-terminal hookworm protein. Sufficient IVTR (600 μ L) for each recombinant protein was prepared to enable intraperitoneal injection of 100 μ L IVTR to each of five mice per group. IVTRs were prepared in RNase/DNase-free 96-well culture plates. Relative fluorescence units (RFU) produced by translation of eGFP-fused recombinant protein in the IVTR was continuously monitored for 2 h on a POLARstar Omega spectrophotometer plate reader (BMG Labtech) at 485-nm excitation and 520-nm emission. IVTRs were centrifuged for 1 min at 300 \times g and the supernatant retained. Protein expression was further validated by sodium dodecyl sulfate polyacrylamide gel electrophoresis (SDS-PAGE) under reducing and nonreducing conditions. Gels were stained for GFP activity using a VersaDoc Imaging System (Bio-Rad) and total IVTR protein content using Colloidal Coomassie.

Recombinant Protein Expression in Human Embryonic Kidney Cells. Select IVTRs that conferred protection in the TNBS colitis model were expressed in Expi293F human embryonic kidney cells (Thermo Fisher). ORFs consisted of the signal peptide from *A. caninum* Ac-ASP-2 (MLVLVPLLALLAVSVHG) followed by the respective ORF (minus the endogenous signal peptide) and a C-terminal 6-His tag. cDNAs were synthesized with mammalian codon bias by Genscript and cloned into the pcDNA3.1 plasmid (Thermo Fisher) by restriction cloning. Plasmids were purified and introduced into Expi293F cells by lipofection using an ExpiFectamine 293 transfection kit (Thermo Fisher) as per the manufacturer's instructions. Recombinant proteins were purified on an AKTA FPLC by immobilized metal affinity chromatography using His-trap excel nickel column and buffer exchanged into tissue culture grade DPBS using Amicon ultra-15 centrifugal concentrators and quantified using a Bicinchoninic Acid kit (Thermo Fisher). Recombinant proteins were assessed for endotoxin using a Limulus Amoebocyte Assay (Thermo Fisher) and only used if endotoxin levels were less than 0.5 endotoxin units per mg protein. Wherever possible, endotoxin-free plasticware was used.

Testing Proteins in the TNBS-Induced Colitis Model. Following anesthesia with 200 mL of 6.25% ketamine (Ketamil; Provect) and 6.25% xylazine (Xylazil; Provect) in PBS, mice were administered intrarectally with 100 μ L of 1.5 mg (5% wt/vol) TNBS solution in 50% EtOH. Test proteins were administered intraperitoneally with 200 mL of 100 mg/mL protein in PBS on day -1 (Fig. 2) or days -1 , $+1$, and $+2$ of the TNBS colitis protocol (Fig. 3). The mice were monitored daily for weight loss and clinical scores (combined from weight loss, piloerection, fecal consistency and mobility, each scored from 0 to 2 except for weight loss which was scored from 0 to 4). Macroscopic scores on day of euthanasia included colon tissue adhesion, ulceration, bowel wall thickening and mucosal edema, each scoring from 0 to 3.

Isolation of Cells from Human Colon Biopsies. Samples were obtained at the Gastroenterology unit of the Prince Charles Hospital in Cherside, QLD. The study designated HREC/2018/QPCH/44524 was approved on 10 October 2018 by the Human Research Ethics Committee at Prince Charles Hospital. Studies

with human samples were acknowledged by the James Cook University Human Research Ethics Committee (H8306). Up to 10 punch biopsies were collected from the colon and stored in 5% fetal bovine serum (FBS) in PBS on ice until further processing. To isolate immune cells, all biopsies from each patient were pooled and placed in Mg²⁺- and Ca²⁺-free Hanks' balanced salt solution supplemented with 5 mM ethylenediaminetetraacetic acid, 1 mM dithiothreitol (DTT), and 5% FBS and incubated for 30 min at 37 °C in a shaking incubator at 250 rpm. The supernatants were collected through a 70-mm strainer, resuspended in RPMI with 10% FBS, and kept on ice until further processing. The remaining tissues were placed in RPMI with 0.2 mg/mL DNase-I (Merck) and 400 U/mL collagenase type I (Gibco) and incubated for 30 min at 37 °C in a shaking incubator at 250 rpm. The samples were then filtered and meshed through a 70-mm cell strainer, resuspended in RPMI with 10% FBS, and combined with the fractions set aside after incubation with DTT.

Human Cytokine Release Assays. A total of 50,000 cells were plated per well in 96-well round bottom plates (Falcon). The cultures were supplemented with 50 µg/mL recombinant protein or CSA, except for Ac-FAR-2, which was added at 10 µg/mL based on previous optimization. Human T-Activator CD3/CD28 Dynabeads (Thermo Fisher) were added according to the manufacturer's recommendation. The cells were incubated at 37 °C, 5% CO₂ overnight, and supernatants were collected and cryopreserved at -80 °C until further processing. For cytokine release analysis the supernatants were thawed on ice and analyzed using a Legendplex Human Inflammation Panel I kit (Biolegend) as per the manufacturer's recommendations.

Cytotoxicity Assay. The lead proteins Ac07727, Ac08034, and Ac-FAR-2 were tested for cytotoxic effects on human PBMC from two healthy donors (James Cook University human ethics approval number H8523 and Australian Red Cross agreement number 21-10QLD-06). CellTox Green cytotoxicity assay was performed according to the manufacturer's instruction, with some adjustments. PBMCs (1 × 10⁶/mL) cultured in 1:1,000 CellTox Green dye medium (Promega) were treated with either PBS, purified recombinant hookworm proteins, or lysis buffer for 18 h at 37 °C and 5% CO₂. Lead recombinant proteins, Ac07727 and Ac08034, were used at 100, 50, and 25 µg/mL Ac-FAR-2 was used at 20, 10, and 5 µg/mL based on earlier studies. Positive control cells were treated with 4% lysis buffer or were left untreated (PBS). Samples containing dye medium only were included for the subtraction of background fluorescence. After overnight culture, fluorescence (RFU) was measured using a FLUOstar Omega microplate reader with an excitation filter of 485-12 and an emission filter of 520. A gain adjustment of 500 was applied. Background fluorescence was subtracted from all readings for analysis, and the mean values ± SD were plotted using GraphPad Prism version 9.3.1.

Fluorescence-Based Binding Assays. Lipid binding by proteins was detected spectrofluorometrically in a PerkinElmer instrument, using *all-trans* retinol or the fluorescent fatty acid analog DAUDA, which bears the environment-sensitive dansyl fluorophore, the intrinsically fluorescent natural fatty acid cPnA, or the non-specific hydrophobic probe ANS. DAUDA and cPnA were obtained from Molecular Probes/Invitrogen and all other compounds were obtained from Sigma. The excitation wavelengths were 345 nm, 350 nm, 319 nm, and 390 nm for DAUDA, retinol, cPnA, and ANS, respectively, which were at concentrations of 1 µM, 4 µM, 4 µM, and 10 µM, respectively, in 2 mL PBS, pH 7.2, in a quartz cuvette. Emission spectra were recorded over wavelength ranges appropriate for each fluorophore to encompass peak emission in water and any shift upon entry into a binding site. Competitive displacement of fluorescent lipids was detected by a reversal of fluorescence enhancement upon addition of the ligand to a preformed complex of protein and fluorescent probe. The fluorescence spectra are uncorrected and were analyzed using MICROCAL ORIGIN software. All proteins were at a concentration of 1 mg/mL and added to the cuvette in 10- or 20-µL amounts. Oleic and arachidonic acids competitors were added in 10-µL amounts to the cuvettes to yield approximate concentrations in the micromolar range in the cuvette and a series of 10-fold increasing concentration increments in competitive displacement experiments.

Statistical Analysis. Data were analyzed using GraphPad Prism 9.0. Comparison of data to control populations (Figs. 2 A-C and 3 A-C) was performed by Mann-Whitney *U* test. Normalized data (Fig. 4) were compared to 100% by one-sample *t* test. Technical errors were removed from data prior to analysis. Sample sizes and statistical analysis methods are indicated in the figure legends.

To assess the performance of IVTRs in the TNBS colitis model (Fig. 2D), we generated combined clinical Z-scores. The raw data of the four outcomes were used to calculate a combined Z-score (SI Appendix, Fig. S3). The Z-score transformation combined the four major outcomes of TNBS colitis—percent of starting weight on day 3 (weight change), macroscopic pathology, clinical score and colon length—per mouse within a group of five mice treated with the same IVTR. The Z-score transformed the raw data into units of SD and showed whether the value of the raw score was below or above the population mean. In this case, the transformation reflected the number of SDs of the raw score of a given colitis parameter for a test group of mice was from the mean of the whole population in the screen. When the population mean scores of both the test (hookworm protein-containing IVTR) and respective experimental negative control (eGFP only IVTR) groups were the same value then the Z-score was zero. A positive Z-score was when the test group mean was higher than the negative control group mean. The four assessed parameters were summed to produce the combined Z-score value, which was compared to the negative control group of each experiment using a two-tailed Student's *t* test with two-sample unequal variance (heteroscedastic). The determined *P* value then allowed each test group to be compared against others across the entire screen.

To assess -log₁₀ *P* value, day-3 colon length and weight loss raw scores from test groups (hookworm protein IVTRs) were compared to the control (eGFP IVTR) group, and significance was determined by a two-sample *t* test. Macroscopic score and clinical score raw data scores from test groups were compared to the control group and significance was determined by a Mann-Whitney *U* test. We adjusted resultant *P* values for multiple testing and transformed the four outcomes to produce the geometric mean of *P* value for each experiment. The geometric mean was chosen because it is less likely to be influenced by outliers and therefore would not skew the ranking of overall efficacy. The significance of the geometric mean of test groups compared to the control group was determined.

Data, Materials, and Software Availability. All study data are included in the article and/or supporting information.

ACKNOWLEDGMENTS. We thank Marcela Montes de Oca, Fabian Rivera, Severine Navarro, Julia Seifert, and Ashley van Waardenberg for technical assistance. We thank Leisa McCann, Myat Myat Khaing, Lei Lin, Ei Swe, and Ann Vandeleur, who helped with clinical investigations.

Author affiliations: ^aAustralian Institute of Tropical Health and Medicine, James Cook University, Cairns, QLD 4878, Australia; ^bCommonwealth Scientific and Industrial Research Organisation-Queensland University of Technology Synthetic Biology Alliance, Australian Research Council Centre of Excellence in Synthetic Biology, Centre for Agriculture and the Bioeconomy, Centre for Genomics and Personalised Health, School of Biology and Environmental Science, Queensland University of Technology, Brisbane, QLD 4000, Australia; ^cInstitute of Biodiversity, Animal Health & Comparative Medicine, College of Medical, Veterinary and Life Sciences, University of Glasgow, Glasgow G12 8QQ, United Kingdom; ^dInstitute of Molecular, Cell and Systems Biology, College of Medical, Veterinary & Life Sciences, University of Glasgow, Glasgow G12 8QQ, United Kingdom; ^eClinical and Health Sciences, University of South Australia, Adelaide, SA 5001, Australia; ^fDivision of Infectious Diseases, QIMR Berghofer Medical Research Institute, Brisbane, QLD 4006, Australia; ^gDivision of Infectious Diseases, Department of Medicine, Washington University in St. Louis, St. Louis, MO 63110; and ^hDepartment of Gastroenterology and Hepatology, Prince Charles Hospital, Brisbane, QLD 4032, Australia

Author contributions: S.M.R., R.R., W.A.J., D.A.P., M.W.K., B.O.S., R.Y.M.R., T.R., K.A., P.R.G., and A.L. designed research; S.M.R., R.R., W.A.J., D.A.P., M.W.K., B.O.S., L.J., G.B., C.P.M., D.J.B., M.M.C., R.Y.M.R., K.M., M.M., and P.R.G. performed research; W.A.J., M.A.F., A.J.E., M.M.C., D.L.D., C.R.E., J.C., T.R., and K.A. contributed new reagents/analytic tools; S.M.R., R.R., W.A.J., D.A.P., M.W.K., B.O.S., M.A.F., M.M.C., R.Y.M.R., P.R.G., and A.L. analyzed data; and S.M.R., R.R., M.W.K., P.R.G., and A.L. wrote the paper.

Competing interest statement: S.M.R., R.R., P.R.G., and A.L. are coinventors on a provisional patent application (AU 2021900769). A.L. and P.R.G. are founders and shareholders of Macrobiome Therapeutics, which is developing hookworm-derived proteins and drugs treating inflammatory conditions.

1. Anonymous; GBD 2017 Inflammatory Bowel Disease Collaborators, The global, regional, and national burden of inflammatory bowel disease in 195 countries and territories, 1990-2017:

A systematic analysis for the Global Burden of Disease Study 2017. *Lancet Gastroenterol. Hepatol.* 5, 17-30 (2020).

2. T. Zuo, M. A. Kamm, J. F. Colombel, S. C. Ng, Urbanization and the gut microbiota in health and inflammatory bowel disease. *Nat. Rev. Gastroenterol. Hepatol.* **15**, 440–452 (2018).
3. M. Coskun, S. Vermeire, O. H. Nielsen, Novel targeted therapies for inflammatory bowel disease. *Trends Pharmacol. Sci.* **38**, 127–142 (2017).
4. G. R. D'Haens, R. B. Sartor, M. S. Silverberg, J. Petersson, P. Rutgeerts, Future directions in inflammatory bowel disease management. *J. Crohn's Colitis* **8**, 726–734 (2014).
5. S. Danese, L. Vuitton, L. Peyrin-Biroulet, Biologic agents for IBD: Practical insights. *Nat. Rev. Gastroenterol. Hepatol.* **12**, 537–545 (2015).
6. K. Yeshi *et al.*, Revisiting inflammatory bowel disease: Pathology, treatments, challenges and emerging therapeutics including drug leads from natural products. *J. Clin. Med.* **9**, 1273 (2020).
7. A. Loukas *et al.*, Hookworm infection. *Nat. Rev. Dis. Primers* **2**, 16088 (2016).
8. R. M. Maizels, H. H. Smits, H. J. McSorley, Modulation of host immunity by helminths: The expanding repertoire of parasite effector molecules. *Immunity* **49**, 801–818 (2018).
9. M. Heylen *et al.*, Of worms, mice and man: An overview of experimental and clinical helminth-based therapy for inflammatory bowel disease. *Pharmacol. Ther.* **143**, 153–167 (2014).
10. S. K. Garg, A. M. Croft, P. Bager, Helminth therapy (worms) for induction of remission in inflammatory bowel disease. *Cochrane Database Syst. Rev.* (1):CD009400. (2014).
11. J. Croese *et al.*, Experimental hookworm infection and gluten microchallenge promote tolerance in celiac disease. *J. Allergy Clin. Immunol.* **135**, 508–516 (2015).
12. J. Croese *et al.*, Randomized, placebo controlled trial of experimental hookworm infection for improving gluten tolerance in celiac disease. *Clin. Transl. Gastroenterol.* **11**, e00274 (2020).
13. S. M. Ryan, R. M. Eichenberger, R. Ruscher, P. R. Giacomin, A. Loukas, Harnessing helminth-driven immunoregulation in the search for novel therapeutic modalities. *PLoS Pathog.* **16**, e1008508 (2020).
14. B. J. Datu *et al.*, Transcriptional changes in the hookworm, *Ancylostoma caninum*, during the transition from a free-living to a parasitic larva. *PLoS Negl. Trop. Dis.* **2**, e130 (2008).
15. J. Mulvenna *et al.*, Proteomics analysis of the excretory/secretory component of the blood-feeding stage of the hookworm, *Ancylostoma caninum*. *Mol. Cell. Proteomics* **8**, 109–121 (2009).
16. I. B. Ferreira *et al.*, Suppression of inflammation and tissue damage by a hookworm recombinant protein in experimental colitis. *Clin. Transl. Immunology* **6**, e157 (2017).
17. J. Meenan *et al.*, Attenuation of the inflammatory response in an animal colitis model by neutrophil inhibitory factor, a novel beta 2-integrin antagonist. *Scand. J. Gastroenterol.* **31**, 786–791 (1996).
18. P. Giuffrida, G. R. Corazza, A. Di Sabatino, Old and new lymphocyte players in inflammatory bowel disease. *Dig. Dis. Sci.* **63**, 277–288 (2018).
19. A. Di Sabatino, M. V. Lenti, P. Giuffrida, A. Vanoli, G. R. Corazza, New insights into immune mechanisms underlying autoimmune diseases of the gastrointestinal tract. *Autoimmun. Rev.* **14**, 1161–1169 (2015).
20. M. F. Rey-Burusco *et al.*, Diversity in the structures and ligand-binding sites of nematode fatty acid and retinol-binding proteins revealed by Na-FAR-1 from *Necator americanus*. *Biochem. J.* **471**, 403–414 (2015).
21. L. O. Perucci *et al.*, Annexin A1 and specialized proresolving lipid mediators: Promoting resolution as a therapeutic strategy in human inflammatory diseases. *Expert Opin. Ther. Targets* **21**, 879–896 (2017).
22. M. A. Liz *et al.*, A narrative review of the role of transthyretin in health and disease. *Neurol. Ther.* **9**, 395–402 (2020).
23. R. J. Hurst, K. J. Else, The retinoic acid-producing capacity of gut dendritic cells and macrophages is reduced during persistent *T. muris* infection. *Parasite Immunol.* **35**, 229–233 (2013).
24. R. J. Hurst, K. J. Else, The retinoic acid-producing capacity of gut dendritic cells and macrophages is reduced during persistent *T. muris* infection. *Parasite Immunol.* **35**, 229–233 (2013).
25. C. D. Funk, Prostaglandins and leukotrienes: Advances in eicosanoid biology. *Science* **294**, 1871–1875 (2001).
26. T. Gobetti, S. N. Cooray, Annexin A1 and resolution of inflammation: Tissue repairing properties and signalling signature. *Biol. Chem.* **397**, 981–993 (2016).
27. G. Leoni *et al.*, Annexin A1-containing extracellular vesicles and polymeric nanoparticles promote epithelial wound repair. *J. Clin. Invest.* **125**, 1215–1227 (2015).
28. M. de Paula-Silva *et al.*, Role of the protein annexin A1 on the efficacy of anti-TNF treatment in a murine model of acute colitis. *Biochem. Pharmacol.* **115**, 104–113 (2016).
29. S. V. Basavaraju *et al.*, Ac-FAR-1, a 20 kDa fatty acid- and retinol-binding protein secreted by adult *Ancylostoma caninum* hookworms: Gene transcription pattern, ligand binding properties and structural characterisation. *Mol. Biochem. Parasitol.* **126**, 63–71 (2003).
30. Z. Hu, Y. J. Bang, K. A. Ruhn, L. V. Hooper, Molecular basis for retinol binding by serum amyloid A during infection. *Proc. Natl. Acad. Sci. U.S.A.* **116**, 19077–19082 (2019).
31. Y. J. Bang *et al.*, Serum amyloid A delivers retinol to intestinal myeloid cells to promote adaptive immunity. *Science* **373**, eabf9232 (2021).
32. Y. T. Tang *et al.*, Genome of the human hookworm *Necator americanus*. *Nat. Genet.* **46**, 261–269 (2014).
33. M. Moyle *et al.*, A hookworm glycoprotein that inhibits neutrophil function is a ligand of the integrin CD11b/CD18. *J. Biol. Chem.* **269**, 10008–10015 (1994).
34. L. Tribolet *et al.*, Probing of a human proteome microarray with a recombinant pathogen protein reveals a novel mechanism by which hookworms suppress B-cell receptor signaling. *J. Infect. Dis.* **211**, 416–425 (2015).
35. O. A. Asojo *et al.*, Heligmosomoides polygyrus venom allergen-like Protein-4 (HpVAL-4) is a sterol binding protein. *Int. J. Parasitol.* **48**, 359–369 (2018).
36. C. D. Buckley *et al.*, Immune-mediated inflammation across disease boundaries: Breaking down research silos. *Nat. Immunol.* **22**, 1344–1348 (2021).
37. S. Mureev, O. Kovtun, U. T. Nguyen, K. Alexandrov, Species-independent translational leaders facilitate cell-free expression. *Nat. Biotechnol.* **27**, 747–752 (2009).